

000 STEP-AWARE POLICY OPTIMIZATION FOR REASON- 001 002 ING IN DIFFUSION LARGE LANGUAGE MODELS 003 004

005 **Anonymous authors**

006 Paper under double-blind review

007 008 ABSTRACT 009

010 Diffusion language models (dLLMs) offer a promising non-autoregressive
011 paradigm for text generation, but training them for complex reasoning remains
012 challenging. Current reinforcement learning approaches typically rely on sparse,
013 outcome-based rewards, which can lead to inefficient exploration and “unstruc-
014 tured refinement”, where the model’s iterative denoising steps fail to contribute
015 meaningfully to the solution. While Process Reward Models (PRMs) effectively
016 mitigate similar issues in autoregressive models, they often require expensive hu-
017 man annotation or external verifiers. **In this work, we propose Step-Aware Policy**
018 **Optimization (SAPO), a method to derive automatic process rewards for dLLMs**
019 **without external supervision.** By leveraging the diffusion model’s natural opera-
020 tion, we design a reward function that incentivizes distributing problem com-
021 plexity evenly across the denoising trajectory. This intrinsic process supervision
022 guides the model to learn structured, robust reasoning paths, reducing the risk of
023 derailing from correct traces. Our empirical results demonstrate that SAPO signif-
024 icantly improves performance on challenging reasoning benchmarks and enhances
025 the interpretability of the generation process.

026 027 1 INTRODUCTION

028 Diffusion large language models (dLLMs) have emerged as a compelling alternative to traditional
029 autoregressive models (ARMs), offering the potential to significantly speed up model inference
030 through their parallel, non-sequential generation process (Nie et al., 2025; Sahoo et al., 2024; Gong
031 et al., 2024; Ye et al., 2025). In particular, mask-based dLLMs (MdLLMs) initialize a sequence with
032 special token [MASK] and iteratively refine this sequence into coherent text. While this paradigm
033 has shown promise on various general tasks, effectively training MdLLMs for complex, multi-step
034 reasoning remains a significant challenge.

035 In the realm of autoregressive models, Process Reward Models (PRMs) (Uesato et al., 2022; Light-
036 man et al., 2023) have become an effective solution for improving reasoning. By providing dense,
037 step-by-step supervision rather than a single sparse reward at the end, PRMs encourage models to
038 maintain coherent reasoning throughout the generation. However, obtaining such dense supervision
039 is costly, often requiring large-scale human annotation or external verifiers. Consequently, current
040 reinforcement learning (RL) methods for MdLLMs, such as GRPO (Shao et al., 2024) adapted in
041 diffu-GRPO (Zhao et al., 2025), typically rely solely on sparse, outcome-based rewards.

042 This reliance on sparse rewards can be problematic. Without intermediate guidance, models are
043 prone to what we term *unstructured refinement*. While models may maintain local textual coherence,
044 they often fail to utilize the iterative denoising process for logical progression. This results in the
045 model wasting steps on unproductive tokens—manifesting as repetitive loops (mode collapse) or
046 coherent but vacuous ‘fluff’—forcing the final few steps to bridge the entire complexity gap. This not
047 only inefficiently uses the diffusion process but also increases the risk of generating hallucinations
048 or inconsistent reasoning paths that only coincidentally arrive at the correct answer (Figure 1).

049 To address this gap, we propose **Step-Aware Policy Optimization (SAPO)**, an algorithm that ex-
050 tracts automatic process rewards for dLLMs. Our key insight is that we can leverage the unique,
051 inherent iterative structure of diffusion models to provide this supervision without external costs.
052 We introduce a method to estimate the contribution of specific denoising intervals by comparing the
053 expected outcome of intermediate states. This allows us to reward denoising steps that demonstrably

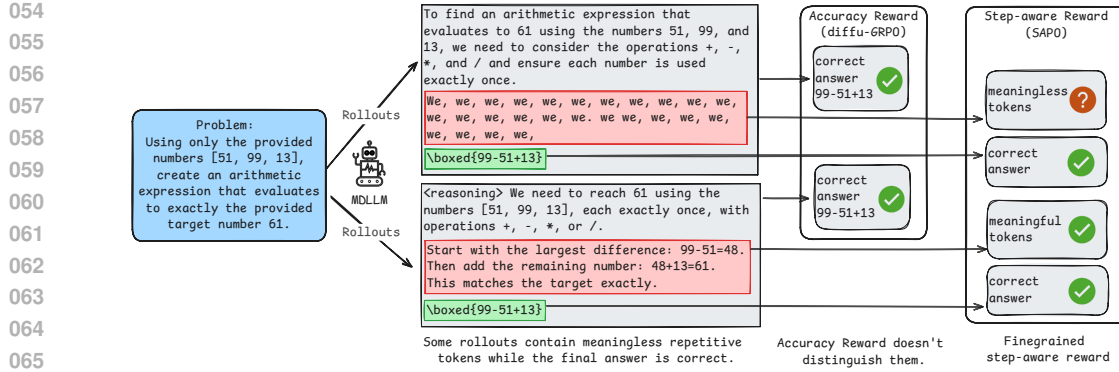


Figure 1: The problem of *unstructured refinement*. A standard MdLLM trained with outcome-only rewards produces a correct answer but fills its reasoning trace with meaningless tokens. While this specific example exhibits mode collapse (a coherence failure), it serves as a stark illustration of a broader issue: the iterative process is not incentivized to reduce problem complexity, allowing the model to ‘spin’ on unproductive steps while coincidentally hitting the correct answer.

reduce the remaining problem complexity, providing a dense supervision signal entirely from within the model’s own rollouts.

This approach serves as a self-supervised mechanism to align the diffusion process with effective reasoning structures. By incentivizing incremental progress, we encourage the model to distribute the problem-solving load across the entire generation process, mitigating the risks associated with unstructured refinement.

Our contributions are as follows:

1. We identify the lack of process supervision as a key limitation in existing MdLLM training, leading to inefficient and potentially unstable reasoning processes.
2. We introduce SAPO, a novel RL framework that provides automatic process rewards for dLLMs. It leverages the diffusion model’s natural operation to incentivize progressive complexity reduction without needing external reward models or verifiers.
3. We demonstrate empirically that SAPO leads to significant improvements in both final performance and the quality of generated reasoning paths across multiple benchmarks, validating the effectiveness of intrinsic process supervision.

2 RELATED WORK

Mask-based diffusion-based large language models. LLaDA (Nie et al., 2025) proposes a mask-based diffusion-based large language model (dLLMs). It gradually removes the mask token in each diffusion step. Based on LLaDA, diffeu-GRPO (Zhao et al., 2025) assumes the generated tokens are independent and proposes a randomly masked prompt to estimate the token probability for reinforcement learning with diffusion models. WINO (Hong et al., 2025) proposes a training-free sampling strategy to use a low confidence threshold to generate a draft response and use a high threshold for second verification. TSE (Wang et al., 2025c) observes that the answers generated in intermediate diffusion steps can also be correct and therefore proposes a weighted voting strategy to get the final answer. ReMDM (Wang et al., 2025a) proposes a remasking sampler to address the problem that the generated tokens in dLLMs cannot be revoked. wd1 (Tang et al., 2025) proposes a weighted likelihood estimation for the sequence. Many approaches have been proposed to improve the efficiency of dLLMs, such as KV-cache (Wu et al., 2025; Song et al., 2025; Liu et al., 2025b; Ma et al., 2025). MDLM (Sahoo et al., 2024) derives a continuous-time, Rao-Blackwellized objective for training mask-based dLLM. LongLLaDA (Liu et al., 2025a) proposes an NTK-based RoPE extrapolation to allow long-context text generation. DiffuCoder (Gong et al., 2025) proposes a coupled sampling scheme to estimate the likelihood for GRPO training. MDPO (He et al., 2025) introduces a running confidence remasking strategy to allow low-confidence tokens to be remasked again during inference time.

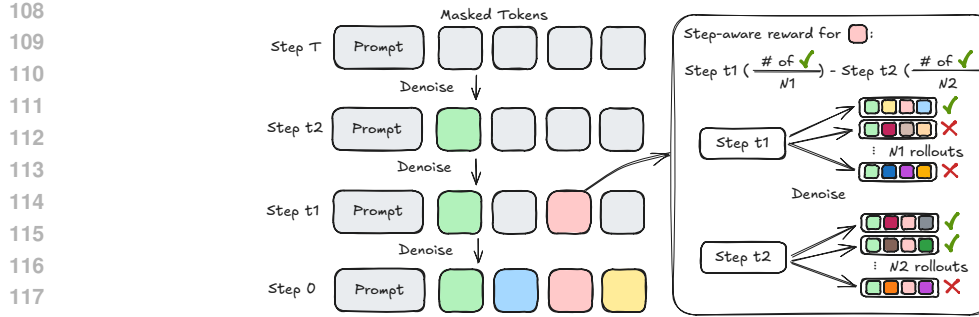


Figure 2: Illustration of the proposed step-aware reward. To encourage intermediate generations to contribute meaningfully to the final outcome, we generate new rollouts from randomly selected steps t_1, t_2 and estimate their contribution by the difference in outcome rewards. A larger difference indicates a higher contribution toward the final correct answer.

Process reward model. Verification models have been shown to improve the multi-step reasoning ability of LLMs. Unlike the outcome verifier (Cobbe et al., 2021; Yu et al., 2023) which examines the correctness of the final outcome, the process reward models enhance feedback accuracy by identifying and localizing errors within generated responses. However, collecting step-wise feedback can be costly, especially with human annotators (Uesato et al., 2022; Lightman et al., 2023). Therefore, many efforts have been devoted to the automatic extraction of process rewards. One standard way to assess process correctness is by estimating, via Monte Carlo (MC) methods, the empirical probability of reaching the correct final answers. Given an intermediate step of reasoning, MATH-SHEPHERD (Wang et al., 2023) asks completers to finalize multiple subsequent reasoning processes and estimate the potential of this step based on the correctness of all decoded answers. (Luo et al., 2024) proposes a Monte Carlo Tree Search algorithm to identify the first error in the reasoning process. (Zhang et al., 2025) argues that the MC-based estimation can be noisy and requires an additional LLM-as-judge to filter the process reward data. Inspired by (Wang et al., 2023), (Wang et al., 2025b) constructs process rewards for multi-modal LLMs. (Zhang et al., 2024a) proposes a tree search policy with process rewards. Implicit process rewards (Yuan et al., 2024; Cui et al., 2025) trains the outcome reward model and can obtain the token-level process reward as log-likelihood ratios of the policy and reference models.

3 STEP-AWARE POLICY OPTIMIZATION FOR STRUCTURED REASONING

Our primary goal is to mitigate the risk of inefficient or derailed reasoning in MdLLMs. We achieve this by providing dense, process-level supervision that encourages the model to distribute problem complexity evenly across generation steps. To obtain this supervision without external annotators or reward models, we leverage the diffusion model’s own iterative nature.

We introduce Step-Aware Policy Optimization (SAPO), a reinforcement learning framework built upon Group Relative Policy Optimization (GRPO) specifically adapted for MdLLMs. Its core innovation is a novel, automatic process-based reward function.

3.1 PRELIMINARY: GROUP RELATIVE POLICY OPTIMIZATION (GRPO)

GRPO is a powerful on-policy algorithm for enhancing the capabilities of language models (Shao et al., 2024). We adapt it for the MdLLM setting.

Response sampling. Given a question Q , we use the current policy π_θ to generate G candidate responses $\{\mathbf{R}^{(1)}, \mathbf{R}^{(2)}, \dots, \mathbf{R}^{(G)}\}$. Each response $\mathbf{R}^{(i)}$ is assigned a reward r_i , based on the correctness of the final answer. From these, we can compute a mean-normalized advantage for each response, $A_i = r_i - \text{mean}(\{r_j\}_{j=1}^G)$. This advantage is distributed across all tokens in the response.

Learning objective. The optimization follows the standard proximity policy optimization (PPO) (Schulman et al., 2017)-style clipped objective for stable updates, regularized by a KL-

162 divergence term against a reference policy π_{ref} :
 163

$$\begin{aligned} \mathcal{L}_{\text{GRPO}}(\theta) = & \mathbb{E}_{\mathbf{Q} \sim \mathcal{D}, \mathbf{R}^{(1)}, \dots, \mathbf{R}^{(G)} \sim \pi_{\theta}(\cdot | \mathbf{Q})} \left[\frac{1}{G} \sum_{i=1}^G \frac{1}{|\mathbf{R}^{(i)}|} \sum_{k=1}^{|\mathbf{R}^{(i)}|} \min \left(\rho_i^k A_i, \text{clip}(\rho_i^k, 1 - \varepsilon, 1 + \varepsilon) A_i \right) \right. \\ & \left. - \beta D_{\text{KL}}[\pi_{\theta}(\cdot | \mathbf{Q}) \| \pi_{\text{ref}}(\cdot | \mathbf{Q})] \right], \end{aligned} \quad (1)$$

170 where the likelihood ratio for the k -th token of response $\mathbf{R}^{(i)}$ is $\rho_i^k = \frac{\pi_{\theta}(\mathbf{R}^{(i),k} | \mathbf{Q}, \mathbf{R}^{(i),<k})}{\pi_{\theta_{\text{old}}}(\mathbf{R}^{(i),k} | \mathbf{Q}, \mathbf{R}^{(i),<k})}$. A key
 171 challenge in applying this to MdLLMs is estimating the sequence likelihood $\pi_{\theta}(\mathbf{R}^{(i)} | \mathbf{Q})$, which
 172 we address with existing techniques (Zhao et al., 2025; Gong et al., 2025; Tang et al., 2025).
 173

174 3.2 STEP-AWARE STRUCTURED REFINEMENT FOR MdLLMs

175 Standard GRPO for MdLLMs defines the advantage A_i based solely on outcome-based rewards
 176 (e.g., final answer accuracy). This may lead to unstructured refinement, as it can equally reinforce
 177 responses that are correct by chance despite having flawed reasoning as illustrated in Fig.1. To
 178 enforce a structured reasoning process, we introduce a step-aware reward.
 179

180 **Denoising steps in MdLLMs.** Given an input question \mathbf{Q} , MdLLM begins by preparing a sequence
 181 of mask tokens `[mask]` of pre-defined length and initializing the denoising process at step $t = T$.
 182 At each iteration, the model receives the partially masked sequence and incrementally replaces mask
 183 tokens with decoded tokens according to a chosen decoding strategy (e.g., decoding only those
 184 tokens whose confidence exceeds a specified threshold). At an intermediate step t , the sequence
 185 thus contains a mixture of text and mask tokens, such as “an apple `[mask]` `[mask]` is on the
 186 `[mask]`”. When $t = 0$, all mask tokens `[mask]` are fully resolved into text tokens.
 187

188 **Evaluating denoising steps with step-aware reward.** To encourage structured reasoning within the
 189 denoising process, one possible approach is to manually annotate intermediate generations, following
 190 the methodology of process reward models developed for ARMs (Uesato et al., 2022). However,
 191 unlike ARMs, where tokens are decoded sequentially and intermediate outputs are inherently struc-
 192 tured and separable, annotating intermediate states in MdLLMs poses additional challenges. This
 193 difficulty arises because MdLLM intermediate generations consist of a mixture of text and mask
 194 tokens, often arranged in a non-deterministic order due to the parallel decoding mechanism. For
 195 instance, an intermediate state might appear as “an apple `[mask]` `[mask]` is on the `[mask]`”,
 196 where incomplete decoding obscures clear annotation.

197 To address this challenge, we propose measuring the incremental progress achieved between dif-
 198 ferent stages of the denoising process. Specifically, we randomly sample two denoising timesteps,
 199 t_1 and t_2 , such that $0 \leq t_1 < t_2 \leq T$. Let x_{t_1} and x_{t_2} denote the intermediate generations at
 200 these steps. To evaluate the contribution of the denoising steps between t_2 and t_1 , we generate full
 201 response rollouts from each state, yielding $\{\mathbf{R}^{(j)}(x_{t_1})\}_{j=1}^{N_1}$ and $\{\mathbf{R}^{(j)}(x_{t_2})\}_{j=1}^{N_2}$.
 202

203 The step-aware reward is defined as the difference in the expected outcome rewards:
 204

$$R_{\text{process}}(t_1, t_2) = \frac{1}{N_1} \sum_{j=1}^{N_1} \mathbf{1}[\mathbf{R}^{(j)}(x_{t_1})] - \frac{1}{N_2} \sum_{j=1}^{N_2} \mathbf{1}[\mathbf{R}^{(j)}(x_{t_2})], \quad (2)$$

205 where $\mathbf{1}[\cdot]$ denotes an indicator function that evaluates the correctness of the final response. A
 206 positive value of R_{process} indicates that the denoising steps between t_2 and t_1 made a meaningful
 207 contribution, thereby reducing its complexity. Importantly, this formulation eliminates the need to
 208 manually annotate intermediate diffusion states or to design task-specific process reward models.
 209

210 **Efficient reward estimation.** Although MdLLMs offer faster inference compared to ARMs, gen-
 211 erating multiple responses from intermediate states at two different timesteps can still be computa-
 212 tionally expensive. To mitigate this cost, we focus on an important special case where $t_2 = T$. At
 213 this point, the intermediate generation x_{t_2} consists entirely of mask tokens `[mask]` ... `[mask]`.
 214 Consequently, the second term $\frac{1}{N_2} \sum_{j=1}^{N_2} \mathbf{1}[\mathbf{R}^{(j)}(x_{t_2})]$ in Eq. 2 corresponds to the model’s accu-
 215 racy when conditioned solely on the input question prompt \mathbf{Q} . In this case, we set $t_2 = T$,

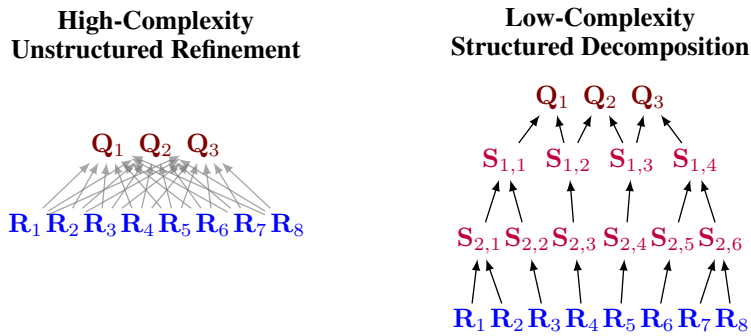


Figure 3: **Complexity reduction via structured decomposition.** (Left) A model without process supervision attempts to solve the complex mapping from Question \mathbf{Q} to Response \mathbf{R} directly, often leading to difficulty bottlenecks. (Right) A model guided by process rewards decomposes the problem into intermediate latent states \mathbf{S} , ensuring each step performs a small, manageable reduction in complexity (sparsity).

$\mathbf{R}^{(j)}(x_{t_2}) = \mathbf{R}^{(j)}$, and $N_2 = G$. Since full response rollouts are already available from GRPO-based accuracy reward computation, this term can be directly estimated without additional inference. In other words, we substitute the mean accuracy reward as a surrogate for the second term, effectively halving the inference cost required to compute $R_{\text{process}}(t_1, t_2)$.

In principle, the full trajectory reward could be computed by evaluating all denoising steps from T down to 0, but this approach would incur prohibitively high computational cost. Instead, we find that estimating the reward using a randomly sampled interval (t_1, t_2) serves as an effective and efficient approximation of the overall reasoning process during generation. Accordingly, we define

$$R_{\text{process}} := R_{\text{process}}(t_1, t_2). \quad (3)$$

Up-weighted advantage computation. In GRPO (Shao et al., 2024) and diffu-GRPO (Zhao et al., 2025), the advantage is computed by normalizing all rewards across rollouts for a given input prompt. However, in our preliminary experiments, we observe that directly applying such normalization to the step-aware reward can degrade model performance. This occurs because samples with $R_{\text{process}} = 0$ are pushed further away during mean-normalization, yielding negative advantages. Such treatment is suboptimal, as these samples (with correct answers and flawed reasoning steps) may still contribute positively to model learning. To address this issue, we introduce an up-weighted strategy for computing the total advantage of response $\mathbf{R}^{(i)}$:

$$A_i^{\text{total}} = A_i + \mathbf{1}[A_i > 0] \cdot R_{\text{process}} \quad (4)$$

where A_i is the advantage for response $\mathbf{R}^{(i)}$. Crucially, up-weighting is applied only to responses that both yield a correct final answer and already possess a positive advantage. This design ensures that we reinforce valid reasoning paths without rewarding intermediate progress that ultimately leads to incorrect solutions, and without penalizing correct answers that may contain imperfect reasoning.

This composite advantage thus integrates correctness with structured, productive reasoning, directly incentivizing the model to adhere to the principle of hierarchical decomposition.

3.3 THEORETICAL UNDERSTANDING: COMPLEXITY DISTRIBUTION

To ground our method in a formal framework, we interpret the benefits of intermediate rewards through the lens of *complexity reduction*. A reasoning task defines a high-complexity constraint between a question \mathbf{Q} and a response \mathbf{R} . Directly generating \mathbf{R} that satisfies \mathbf{Q} without structured guidance is difficult because the search space is vast and the dependency is complex (Figure 3, Left). We do not posit this hierarchical structure as a rigid, universal cognitive model. Rather, we propose the hierarchy as a flexible abstraction for the potential reasoning complexity. Simpler problems activate only a sparse subgraph of the available constraints. In the context of diffusion, this manifests as trivial transformations where the ‘reasoning’ happens implicitly via smooth constraint satisfaction in the latent space, without requiring complex structural decomposition.

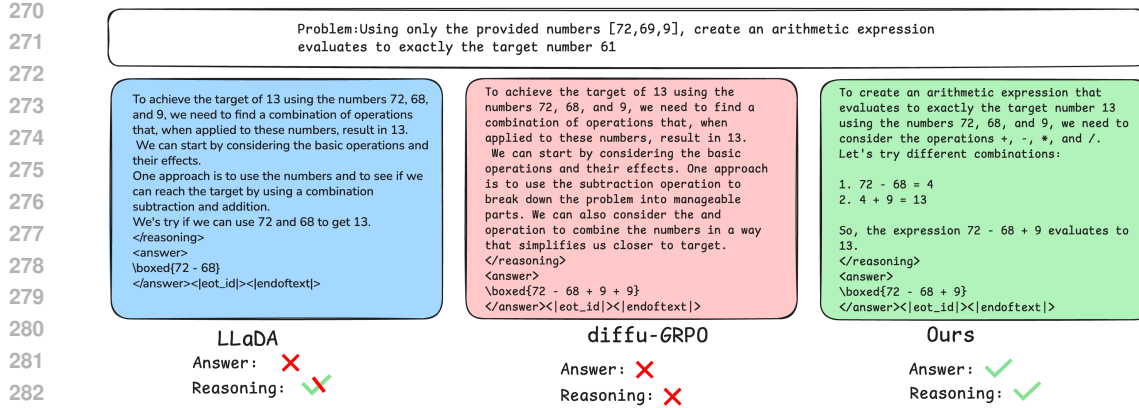


Figure 4: Comparison of generated responses across models. LLaDA (Nie et al., 2025) and diffu-GRPO (Zhao et al., 2025) both produce incorrect answers to the evaluation question. LLaDA’s response includes a brief but partially meaningful reasoning step toward the end, whereas diffu-GRPO continues generating verbose sentences that contribute little to the final prediction. In contrast, our model provides a structured reasoning process and successfully arrives at the correct answer. This highlights that optimizing solely for accuracy-based rewards may lead to sub-optimal outcomes, as such rewards overlook the quality and coherence of reasoning within the response.

Standard dLLM training paradigms are often agnostic to intermediate progress, suffering from **unstructured refinement**: the model may waste early steps on irrelevant tokens or derail from a logical path, forcing it to bridge a massive complexity gap in the final few steps.

Ideally, the difficulty of the problem should decrease monotonically and gradually as the diffusion proceeds. We formally characterize this as a **sparsity constraint** on the latent reasoning process (see Appendix B for details). Intuitively, if a model can decompose a complex function into a composition of sparse, simple functions, it can more easily learn a natural, robust reasoning process.

Theorem 3.1 (Informal: Complexity Distribution). *A reasoning model that distributes the computational load (e.g., satisfies a sparsity constraint), where each transition resolves only a limited subset of dependencies, learns a natural, robust reasoning process that is less prone to unstructured refinement.*

Our proposed method, SAPO, directly operationalizes this insight. By rewarding intervals that show a measurable increase in the probability of correctness, we encourage the model to distribute the complexity reduction evenly across all steps, ensuring that every stage of the diffusion process contributes a small, manageable piece of the solution.

4 EXPERIMENTS

4.1 SETUP

We build our model on top of diffu-GRPO (Zhao et al., 2025) and adopt the same experimental setup unless otherwise specified. We provide implementation details in the Appendix.C.

Datasets. We evaluate on four benchmarks: (1) GSM8K (Cobbe et al., 2021), using 7,374 training and 1,319 test problems; (2) MATH (Lightman et al., 2023), with 7,500 training and 500 test problems; (3) COUNTDOWN, a synthetic dataset of 490K training and 256 test samples requiring arithmetic expression generation; and (4) SUDOKU, 4×4 puzzles evaluated on a 256-sample split.

Baselines. We compare against recent state-of-the-art MdLLMs: LLaDA (Nie et al., 2025), Diffu-GRPO (Zhao et al., 2025), TSE (Wang et al., 2025c), and WINO (Hong et al., 2025), as well as models further fine-tuned on the reasoning dataset s1K (Muennighoff et al., 2025).

Model / Seq Len	COUNTDOWN			GSM8K			SUDOKU			MATH		
	128	256	512	128	256	512	128	256	512	128	256	512
LLaDA	20.7	19.5	16.0	68.7	76.7	78.2	11.7	6.7	5.5	26.0	32.4	36.2
diffu-GRPO	33.2	31.3	37.1	72.6	79.8	81.9	18.4	12.9	11.0	33.2	37.2	39.2
TSE-Vote	25.0	23.4	16.4	70.1	78.7	78.9	×	×	×	28.4	35.6	36.2
WINO	-	33.2	-	-	75.8	-	-	15.2	-	-	34.2	-
SFT	20.3	14.5	23.8	66.5	78.8	81.1	16.5	8.5	4.6	26.2	32.6	34.8
SFT + diffu-GRPO	34.8	32.0	42.2	73.2	81.1	82.1	22.1	16.7	9.5	33.8	38.6	40.2
SFT + TSE-Reward	41.5	42.6	54.7	72.1	80.0	83.0	×	×	×	31.2	35.4	41.4
diffu-GRPO+PRM	-	-	-	71.7	80.9	81.5	-	-	-	30.8	36.0	36.0
Ours	51.6	52.0	56.3	72.9	82.2	82.4	22.4	20.3	16.1	32.0	40.0	38.4

Table 1: Performance comparison on COUNTDOWN, GSM8K, SUDOKU, and MATH at different sequence lengths. “–” denotes unreported results; “×” denotes unsupported tasks. Without additional SFT on the reasoning dataset s1K (Muennighoff et al., 2025), our method achieves superior performance across all four tasks.

Model/Seq Len	COUNTDOWN			sec/it
	128	256	512	
diffu-GRPO	33.2	31.3	37.1	3.19
diffu-GRPO+PRM	-	-	-	7.58
Ours-NoUpweight	41.0	41.4	50.4	3.42
Ours-Cover	55.1	59.4	58.2	6.23
Ours-Random	55.4	54.7	59.8	4.76
Ours	51.6	52.0	56.3	3.42

Table 2: Ablation on different designs and efficiency comparisons.

Dataset	diffu-GRPO	Ours
COUNTDOWN	4.37 ± 2.41	3.80 ± 2.04
GSM8K	2.37 ± 0.80	2.12 ± 0.74
SUDOKU	4.31 ± 2.95	3.90 ± 2.44
MATH	3.19 ± 1.21	3.11 ± 1.24

Table 3: The number of causal links across timesteps. With the proposed reward, our approach learns a sparser hierarchy (smaller mean), and the changes across timesteps (hierarchy levels) are smoother and more stable, as indicated by the smaller standard deviation.

4.2 RESULTS

Alignment of reasoning process and final answer. To assess how well MDLLMs produce intermediate reasoning that is consistent with the final answer, we analyze the alignment between the reasoning process and the output. Specifically, we input generations from LLaDA (Nie et al., 2025), diffu-GRPO (Zhao et al., 2025), and our model into GPT-5, asking it to evaluate “whether a user can reach the final answer by following the reasoning step by step.” Results on the COUNTDOWN and GSM8K datasets are shown in Fig. 6. Our method achieves substantially higher alignment ratios across both datasets. This large improvement helps explain the performance gains in Table 1, as our proposed reward explicitly encourages the model to maintain consistency between reasoning steps and final answers through the diffusion-based generation process. We also provide example outputs from the three models in Fig. 1. As shown, LLaDA and diffu-GRPO generate less meaningful reasoning in their responses and ultimately produce incorrect answers.

Comparison with using pretrained PRM. Since our approach is fundamentally built upon the idea of process rewards, it is crucial to understand how it compares to an existing and widely adopted paradigm for process-level supervision: using a pretrained Process Reward Model (PRM) as the reward function. To this end, we adopted the pretrained Mistral-7B PRM checkpoint from Zhang et al. (2024b). We inserted their reasoning-step tags every 16 timesteps during masked-token decoding, fed the entire sequence into the PRM, and computed the process reward as the average PRM score across timestep intervals.

Despite PRMs being effective for test-time selection, we encountered several significant challenges when attempting to use them as training-time rewards for dLLM policy optimization as shown in Fig.5: (1) Huge memory consumption. Unlike our approach, which reuses the training model itself to compute rewards, the pretrained PRM introduces substantial GPU and CPU memory overhead, leading to much slower training (7.62 sec/it vs. 3.42 sec/it for ours; see Table 2). (2) Instability. Generated responses frequently caused the PRM to output NaNs, likely because it expects strictly

Model	Training	SVAMP	ARC
LLaDA	-	83.3	90.2
diffu-GRPO	GSM8K	83.0	89.8
Ours	GSM8K	84.0	90.2
diffu-GRPO	MATH	83.7	91.8
Ours	MATH	85.7	93.0
diffu-GRPO	COUNTDOWN	84.0	90.6
Ours	COUNTDOWN	84.0	87.5
diffu-GRPO	SUDOKU	85.0	91.0
Ours	SUDOKU	86.7	90.6

Table 4: Generalization ability comparison. The trained models are evaluated on unseen datasets: the reasoning benchmark SVAMP (Patel et al., 2021) and the commonsense benchmark ARC (Clark et al., 2018).

Step	COUNTDOWN		GSM8K	
	diffu-GRPO	Ours	diffu-GRPO	Ours
1	1.56	1.17	12.81	16.53
8	2.73	1.56	9.48	16.91
16	3.12	2.34	13.04	19.33
24	4.69	1.95	17.21	21.61
32	6.64	27.34	24.26	30.86
40	12.50	33.98	39.27	41.17
48	19.53	37.11	49.96	50.57
64	33.2	51.6	72.6	72.9

Table 5: Accuracy of intermediate answers with sequence length 128 and 64 diffusion steps. Intermediate answers are obtained by decoding normally up to a target step and then decoding all remaining tokens in one pass.

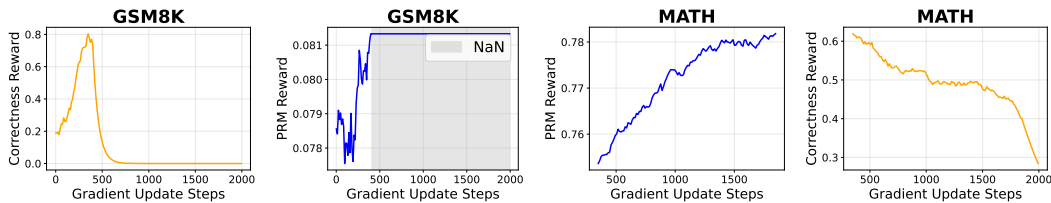


Figure 5: Two failure runs when using a pretrained PRM to assign rewards: instability and potential reward hacking. Unlike our rule-based reward, the PRM must process the full model-generated response through a large pretrained network. As a result, it often encounters unseen or irregular response formats, which can lead to numerical instabilities and NaN outputs. In addition, as shown on the right for the MATH dataset, although the PRM reward steadily increases during training, the accuracy reward actually decreases. This divergence suggests that the model learns to exploit weaknesses in the PRM scoring function—effectively hacking the reward model rather than improving its reasoning quality.

formatted inputs (e.g., explicit “step1/step2” markers). This forced us to replace NaN scores with zero, introducing further noise into the learning process. (3) Reward hacking. Although the PRM reward steadily increased during training, the actual task performance did not improve. This suggests that the policy model learns to exploit flaws in the PRM scoring function rather than improving its reasoning quality—a well-known failure mode for reward-model-based optimization. As shown in Table 1, diffu-GRPO+PRM achieves 71.7, 80.9, and 81.5 on GSM8K, while diffu-GRPO obtains 72.6, 79.8, and 81.9. Our method further improves to 72.9, 82.2, and 82.4. These results underscore that, even when compared against a strong pretrained PRM, our rule-based reward provides more stable optimization and better downstream performance, reinforcing the motivation for our design.

Ablation study on the model design. We now examine several design choices in our framework. Ours-NoUpweight removes the up-weighting strategy and applies the reward to all samples rather than only those with positive advantages. Ours-Cover computes the proposed reward across all timestep intervals, corresponding to the exact empirical average. Ours-Random selects t_2 uniformly at random instead of fixing $t_2 = T$. The results on the COUNTDOWN dataset are shown in Table 2.

The ablation results demonstrate the contributions of each component. Removing the up-weighting strategy (Ours-NoUpweight) already yields notable improvements over diffu-GRPO (e.g., 41.0 vs. 33.2 at sequence length 128), indicating that the reward formulation alone provides a substantial benefit. Computing rewards across all timestep intervals (Ours-Cover) achieves the strongest overall performance (55.1, 59.4, 58.2), but requires roughly twice the computation time (6.23 sec/it). Sampling t_2 at random (Ours-Random) achieves similarly strong accuracy (55.4, 54.7, 59.8), though it is still slower than our approach (4.76 sec/it), as it requires an additional forward pass and cannot reuse the final completion for filtering. Our full method (Ours) achieves performance close to Ours-Cover

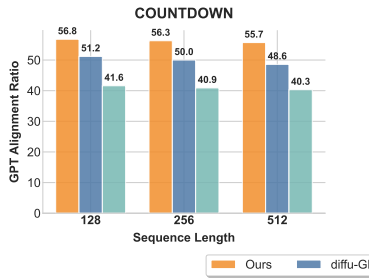


Figure 6: Model reasoning–outcome alignment ratio.

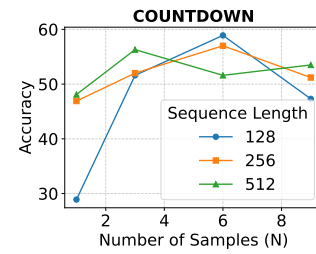


Figure 7: Ablation study.

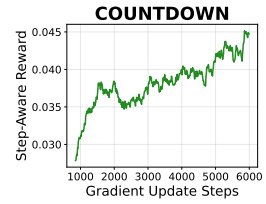


Figure 8: The training curve of our proposed step-aware reward.

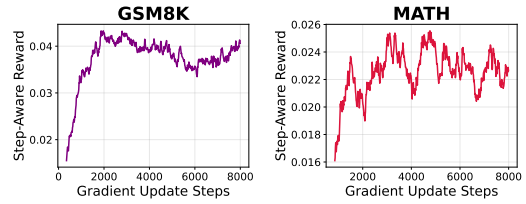


Figure 9: Reward curves during GRPO training. For fair comparison, we exclude our step-aware reward. The step-aware reward emphasizes responses that contain both the correct answer and meaningful reasoning, which in turn enhances the accuracy reward.

452
453
454
455
456
457
458
459
460
461
462
463
464
465
466
467
468
469
470
471
472
473
474
475
476
477
478
479
480
481
482
483
484
485

and Ours-Random (51.6, 52.0, 56.3), while maintaining a training speed comparable to diffu-GRPO (3.42 sec/it vs. 3.19 sec/it). This indicates that our design provides an efficient approximation of the full reward with minimal computational overhead. For completeness, we also report the runtime of diffu-GRPO+PRM (7.58 sec/it), which is substantially slower due to the additional memory and computation required by the pretrained PRM model.

Our reward enables a more sparse and stable reasoning hierarchy. Our theoretical analysis suggests that enforcing suitable sparsity constraints should lead the model to learn a more structured and well-organized reasoning hierarchy. To empirically verify this prediction, we examine the causal structure induced by the learned models. At each prediction step, we estimate the causal links between hierarchy levels using token prediction probabilities. For example, given a partially decoded sequence such as “I am [mask]”, we count how many vocabulary tokens have prediction probability greater than a small threshold (e.g., 0.01), treating each such token as an active causal link. We then compute the average and standard deviation of the number of causal links across timesteps.

As shown in Table 3, our approach consistently produces fewer causal links than diffu-GRPO, indicating a sparser learned hierarchy. For instance, on COUNTDOWN, the number of causal links decreases from 4.37 to 3.80 (a 13.1% reduction), and on SUDOKU it decreases from 4.31 to 3.90 (a 9.5% reduction). Likewise, our model shows smaller standard deviations—e.g., from 2.41 to 2.04 on COUNTDOWN—demonstrating that the changes across hierarchy levels are smoother and more stable. Similar trends hold across GSM8K and MATH. These empirical findings align with our theoretical motivation and confirm that our reward encourages a more structured reasoning process.

Superior benchmark performance. Table 1 reports results on benchmarks: GSM8K, MATH, COUNTDOWN, and SUDOKU. Our approach outperforms baselines across most datasets and even surpasses those fine-tuned with additional reasoning dataset s1K (Muennighoff et al., 2025).

486 **The proposed reward is effectively learned and facilitates training.** We visualize the training re-
 487 wards of diffu-GRPO (Zhao et al., 2025) and our model in Fig. 9. Our method consistently achieves
 488 higher total rewards—which combine both accuracy and format rewards—explaining the substantial
 489 performance gains observed on these datasets. For MATH, however, the training rewards of both
 490 methods remain similar. A similar phenomenon was also reported in (Zhao et al., 2025), where the
 491 diffu-GRPO model after SFT on s1k dataset (Muennighoff et al., 2025) attained rewards similar to
 492 those without SFT. We hypothesize that the MATH500 problems may be too challenging for the
 493 8B base model and may be addressed with a larger dLLM. We further present the reward training
 494 curves in Fig. 8. The upward trend indicates that the model learns to favor responses yielding correct
 495 answers while adhering to reasoning processes that support the final outcome.

496 **Our model demonstrates strong generalization ability.** To thoroughly examine the proposed
 497 framework, we further evaluate our models on two unseen datasets: SVAMP (Patel et al., 2021)
 498 and ARC (Clark et al., 2018). The SVAMP dataset consists of numerous mathematical reasoning
 499 problems, while the ARC dataset focuses on commonsense reasoning tasks (e.g., “When oxygen
 500 combines with hydrogen, which substance is formed?”), where the model must select the correct
 501 answer from multiple choices. Notably, ARC is fundamentally different from our training datasets
 502 (e.g., GSM8K). Our model noticeably improves performance on both SVAMP and ARC.

503 **Our method enables further acceleration through higher intermediate accuracy.** Accelerating
 504 MDLLMs has been an active area of research (Li et al., 2025; Hong et al., 2025; He et al., 2025).
 505 Many approaches rely on the quality of intermediate responses: if these responses are accurate and
 506 contribute meaningfully to the final answer, generation can be accelerated. For instance, Prophet (Li
 507 et al., 2025) decides whether to decode all remaining tokens in a single step. Motivated by this,
 508 we analyze the accuracy of intermediate responses produced by our method. Specifically, during
 509 diffusion denoising, at each step, we additionally generate an answer by unmasking all remaining
 510 tokens at once. This gives us intermediate answers at every step, in addition to the final output
 511 obtained from fully decoding the masked sequence. We present results in Table.5. Across both
 512 datasets, our method achieves higher intermediate accuracy, suggesting that it may offer advantages
 513 over diffu-GRPO (Zhao et al., 2025) when combined with MdLLM acceleration techniques.

514 **Effect of the number of samples on the reward.** Our step-aware reward function is based on an
 515 averaged estimation of the accuracy of generated responses. To assess its reliability, we perform an
 516 ablation study by varying the number of samples, $N \in \{1, 3, 6, 9\}$. As illustrated in Fig. 7, when
 517 $N = 1$, the estimation becomes noisy and leads to suboptimal performance. In contrast, when
 518 $N \geq 3$, we observe substantial improvements over both baseline methods, LLaDA (Nie et al., 2025)
 519 and diffu-GRPO (Zhao et al., 2025), across sequence lengths of 128, 256, and 512. These results
 520 highlight the robustness of our proposed reward under different sampling configurations.

5 CONCLUSION AND LIMITATIONS

521
 522
 523
 524
 525
 526 We address the challenge of training diffusion language models for complex reasoning, identifying
 527 the lack of process supervision as a key limitation that leads to *unstructured refinement*. To over-
 528 come this without incurring the high costs of external verifiers or human annotation, we introduce
 529 SAPO, an RL framework that derives automatic process rewards from the diffusion model’s inherent
 530 iterative structure. Supported by the theoretical insight of progressive complexity reduction, SAPO
 531 incentivizes the model to distribute problem difficulty evenly across the denoising trajectory, fos-
 532 tering structured and robust reasoning. Our empirical results demonstrate that SAPO significantly
 533 improves performance on challenging reasoning benchmarks and enhances the coherence of the
 534 generation process.

535 **Limitation.** Our method relies on the mean-field assumption used in diffu-GRPO (Zhao et al., 2025)
 536 to estimate the log-likelihood of generated responses, which inherently neglects token-level depen-
 537 dencies. Unfortunately, this assumption is difficult to remove because, unlike ARM-based models,
 538 dLLM does not provide a convenient factorization that would allow us to compute likelihoods ex-
 539 actly. For efficiency reasons, we therefore must adopt additional approximations. Addressing this
 540 limitation is an important direction for future work.

540 REFERENCES
541

542 Peter Clark, Isaac Cowhey, Oren Etzioni, Tushar Khot, Ashish Sabharwal, Carissa Schoenick, and
543 Oyvind Tafjord. Think you have solved question answering? try arc, the ai2 reasoning challenge.
544 *arXiv preprint arXiv:1803.05457*, 2018.

545 Karl Cobbe, Vineet Kosaraju, Mohammad Bavarian, Mark Chen, Heewoo Jun, Lukasz Kaiser,
546 Matthias Plappert, Jerry Tworek, Jacob Hilton, Reiichiro Nakano, et al. Training verifiers to
547 solve math word problems. *arXiv preprint arXiv:2110.14168*, 2021.

548 Ganqu Cui, Lifan Yuan, Zefan Wang, Hanbin Wang, Wendi Li, Bingxiang He, Yuchen Fan, Tianyu
549 Yu, Qixin Xu, Weize Chen, et al. Process reinforcement through implicit rewards. *arXiv preprint*
550 *arXiv:2502.01456*, 2025.

551 Shansan Gong, Shivam Agarwal, Yizhe Zhang, Jiacheng Ye, Lin Zheng, Mukai Li, Chenxin An,
552 Peilin Zhao, Wei Bi, Jiawei Han, et al. Scaling diffusion language models via adaptation from
553 autoregressive models. *arXiv preprint arXiv:2410.17891*, 2024.

554 Shansan Gong, Ruixiang Zhang, Huangjie Zheng, Jiatao Gu, Navdeep Jaitly, Lingpeng Kong, and
555 Yizhe Zhang. Diffucoder: Understanding and improving masked diffusion models for code gen-
556 eration. *arXiv preprint arXiv:2506.20639*, 2025.

557 Haoyu He, Katrin Renz, Yong Cao, and Andreas Geiger. Mdpo: Overcoming the training-inference
558 divide of masked diffusion language models. *arXiv preprint arXiv:2508.13148*, 2025.

559 Feng Hong, Geng Yu, Yushi Ye, Haicheng Huang, Huangjie Zheng, Ya Zhang, Yanfeng Wang, and
560 Jiangchao Yao. Wide-in, narrow-out: Revokable decoding for efficient and effective dllms. *arXiv*
561 *preprint arXiv:2507.18578*, 2025.

562 Aapo Hyvärinen and Hiroshi Morioka. Unsupervised feature extraction by time-contrastive learning
563 and nonlinear ica, 2016.

564 Aapo Hyvärinen, Hiroaki Sasaki, and Richard Turner. Nonlinear ica using auxiliary variables and
565 generalized contrastive learning. In *The 22nd International Conference on Artificial Intelligence
566 and Statistics*, pp. 859–868. PMLR, 2019.

567 Lingjing Kong, Shaoan Xie, Weiran Yao, Yujia Zheng, Guangyi Chen, Petar Stojanov, Victor
568 Akinwande, and Kun Zhang. Partial disentanglement for domain adaptation. In Kamalika
569 Chaudhuri, Stefanie Jegelka, Le Song, Csaba Szepesvari, Gang Niu, and Sivan Sabato (eds.),
570 *Proceedings of the 39th International Conference on Machine Learning*, volume 162 of *Pro-
571 ceedings of Machine Learning Research*, pp. 11455–11472. PMLR, 17–23 Jul 2022. URL
572 <https://proceedings.mlr.press/v162/kong22a.html>.

573 Pengxiang Li, Yefan Zhou, Dilxat Muhtar, Lu Yin, Shilin Yan, Li Shen, Yi Liang, Soroush Vosoughi,
574 and Shiwei Liu. Diffusion language models know the answer before decoding. *arXiv preprint*
575 *arXiv:2508.19982*, 2025.

576 Hunter Lightman, Vineet Kosaraju, Yuri Burda, Harrison Edwards, Bowen Baker, Teddy Lee, Jan
577 Leike, John Schulman, Ilya Sutskever, and Karl Cobbe. Let’s verify step by step. In *The Twelfth
578 International Conference on Learning Representations*, 2023.

579 Xiaoran Liu, Zhigeng Liu, Zengfeng Huang, Qipeng Guo, Ziwei He, and Xipeng Qiu. Longllada:
580 Unlocking long context capabilities in diffusion llms. *arXiv preprint arXiv:2506.14429*, 2025a.

581 Zhiyuan Liu, Yicun Yang, Yaojie Zhang, Junjie Chen, Chang Zou, Qingyuan Wei, Shaobo Wang,
582 and Linfeng Zhang. dllm-cache: Accelerating diffusion large language models with adaptive
583 caching. *arXiv preprint arXiv:2506.06295*, 2025b.

584 Liangchen Luo, Yinxiao Liu, Rosanne Liu, Samrat Phatale, Meiqi Guo, Harsh Lara, Yunxuan Li,
585 Lei Shu, Yun Zhu, Lei Meng, et al. Improve mathematical reasoning in language models by
586 automated process supervision. *arXiv preprint arXiv:2406.06592*, 2024.

587 Xinyin Ma, Rupeng Yu, Gongfan Fang, and Xinchao Wang. dkv-cache: The cache for diffusion
588 language models. *arXiv preprint arXiv:2505.15781*, 2025.

594 Niklas Muennighoff, Zitong Yang, Weijia Shi, Xiang Lisa Li, Li Fei-Fei, Hannaneh Hajishirzi, Luke
 595 Zettlemoyer, Percy Liang, Emmanuel Candès, and Tatsunori Hashimoto. s1: Simple test-time
 596 scaling. *arXiv preprint arXiv:2501.19393*, 2025.

597 Shen Nie, Fengqi Zhu, Zebin You, Xiaolu Zhang, Jingyang Ou, Jun Hu, Jun Zhou, Yankai
 598 Lin, Ji-Rong Wen, and Chongxuan Li. Large language diffusion models. *arXiv preprint*
 599 *arXiv:2502.09992*, 2025.

600 Arkil Patel, Satwik Bhattacharya, and Navin Goyal. Are nlp models really able to solve simple math
 601 word problems? *arXiv preprint arXiv:2103.07191*, 2021.

602 Subham Sahoo, Marianne Arriola, Yair Schiff, Aaron Gokaslan, Edgar Marroquin, Justin Chiu,
 603 Alexander Rush, and Volodymyr Kuleshov. Simple and effective masked diffusion language
 604 models. *Advances in Neural Information Processing Systems*, 37:130136–130184, 2024.

605 John Schulman, Filip Wolski, Prafulla Dhariwal, Alec Radford, and Oleg Klimov. Proximal policy
 606 optimization algorithms. *arXiv preprint arXiv:1707.06347*, 2017.

607 Zhihong Shao, Peiyi Wang, Qihao Zhu, Runxin Xu, Junxiao Song, Xiao Bi, Haowei Zhang,
 608 Mingchuan Zhang, YK Li, Yang Wu, et al. Deepseekmath: Pushing the limits of mathematical
 609 reasoning in open language models. *arXiv preprint arXiv:2402.03300*, 2024.

610 Yuerong Song, Xiaoran Liu, Ruixiao Li, Zhigeng Liu, Zengfeng Huang, Qipeng Guo, Ziwei He,
 611 and Xipeng Qiu. Sparse-dllm: Accelerating diffusion llms with dynamic cache eviction. *arXiv*
 612 *preprint arXiv:2508.02558*, 2025.

613 Xiaohang Tang, Rares Dolga, Sangwoong Yoon, and Ilija Bogunovic. wd1: Weighted policy opti-
 614 mization for reasoning in diffusion language models. *arXiv preprint arXiv:2507.08838*, 2025.

615 Jonathan Uesato, Nate Kushman, Ramana Kumar, Francis Song, Noah Siegel, Lisa Wang, Antonia
 616 Creswell, Geoffrey Irving, and Irina Higgins. Solving math word problems with process-and
 617 outcome-based feedback. *arXiv preprint arXiv:2211.14275*, 2022.

618 Guanghan Wang, Yair Schiff, Subham Sekhar Sahoo, and Volodymyr Kuleshov. Remasking discrete
 619 diffusion models with inference-time scaling. *arXiv preprint arXiv:2503.00307*, 2025a.

620 Peiyi Wang, Lei Li, Zhihong Shao, RX Xu, Damai Dai, Yifei Li, Deli Chen, Yu Wu, and Zhifang
 621 Sui. Math-shepherd: Verify and reinforce llms step-by-step without human annotations. *arXiv*
 622 *preprint arXiv:2312.08935*, 2023.

623 Weiyun Wang, Zhangwei Gao, Lianjie Chen, Zhe Chen, Jinguo Zhu, Xiangyu Zhao, Yangzhou Liu,
 624 Yue Cao, Shenglong Ye, Xizhou Zhu, et al. Visualprm: An effective process reward model for
 625 multimodal reasoning. *arXiv preprint arXiv:2503.10291*, 2025b.

626 Wen Wang, Bozhen Fang, Chenchen Jing, Yongliang Shen, Yangyi Shen, Qiuyu Wang, Hao Ouyang,
 627 Hao Chen, and Chunhua Shen. Time is a feature: Exploiting temporal dynamics in diffusion
 628 language models. *arXiv preprint arXiv:2508.09138*, 2025c.

629 Chengyue Wu, Hao Zhang, Shuchen Xue, Zhijian Liu, Shizhe Diao, Ligeng Zhu, Ping Luo, Song
 630 Han, and Enze Xie. Fast-dllm: Training-free acceleration of diffusion llm by enabling kv cache
 631 and parallel decoding. *arXiv preprint arXiv:2505.22618*, 2025.

632 Jiacheng Ye, Zhihui Xie, Lin Zheng, Jiahui Gao, Zirui Wu, Xin Jiang, Zhenguo Li, and Lingpeng
 633 Kong. Dream 7b: Diffusion large language models. *arXiv preprint arXiv:2508.15487*, 2025.

634 Fei Yu, Anningzhe Gao, and Benyou Wang. Ovm, outcome-supervised value models for planning
 635 in mathematical reasoning. *arXiv preprint arXiv:2311.09724*, 2023.

636 Lifan Yuan, Wendi Li, Huayu Chen, Ganqu Cui, Ning Ding, Kaiyan Zhang, Bowen Zhou,
 637 Zhiyuan Liu, and Hao Peng. Free process rewards without process labels. *arXiv preprint*
 638 *arXiv:2412.01981*, 2024.

639 Dan Zhang, Sining Zhoubian, Ziniu Hu, Yisong Yue, Yuxiao Dong, and Jie Tang. Rest-mcts*: Llm
 640 self-training via process reward guided tree search. *Advances in Neural Information Processing*
 641 *Systems*, 37:64735–64772, 2024a.

648 Hanning Zhang, Pengcheng Wang, Shizhe Diao, Yong Lin, Rui Pan, Hanze Dong, Dylan Zhang,
649 Pavlo Molchanov, and Tong Zhang. Entropy-regularized process reward model. *arXiv preprint*
650 *arXiv:2412.11006*, 2024b.

651

652 Zhenru Zhang, Chujie Zheng, Yangzhen Wu, Beichen Zhang, Runji Lin, Bowen Yu, Dayiheng Liu,
653 Jingren Zhou, and Junyang Lin. The lessons of developing process reward models in mathematical
654 reasoning. *arXiv preprint arXiv:2501.07301*, 2025.

655 Siyan Zhao, Devaansh Gupta, Qinqing Zheng, and Aditya Grover. d1: Scaling reasoning in diffusion
656 large language models via reinforcement learning. *arXiv preprint arXiv:2504.12216*, 2025.

657

658 Yujia Zheng, Ignavier Ng, and Kun Zhang. On the identifiability of nonlinear ica: Sparsity and
659 beyond. *arXiv preprint arXiv:2206.07751*, 2022.

660 Yujia Zheng, Shaoan Xie, and Kun Zhang. Nonparametric identification of latent concepts. In *Forty-*
661 *second International Conference on Machine Learning*, 2025. URL <https://openreview.net/forum?id=cW9Ttnm1aC>.

663

664

665

666

667

668

669

670

671

672

673

674

675

676

677

678

679

680

681

682

683

684

685

686

687

688

689

690

691

692

693

694

695

696

697

698

699

700

701

702
703
704
705
706
707
708
709
710
711
712
713
714
715
716
717
718
719
720
721
722
723
724
725
726
727
728
729
730
731
732
733
734
735
736
737
738
739
740
741
742
743
744
745
746
747
748
749
750
751
752
753
754
755

Appendix

A LLM USAGES.

Large Language Models (LLMs) were used solely for polishing the writing and improving the clarity of presentation. All ideas, analyses, results, and conclusions are original contributions of the authors.

B THEORETICAL ANALYSIS

In this section, we provide a theoretical foundation for our work. The central insight is that if the underlying hierarchical structure of reasoning can be learned from data, then there is a principled basis for designing algorithms that explicitly seek this structure. We establish this by showing that the latent concepts at each level of our proposed hierarchy are identifiable up to benign ambiguities.

B.1 IDENTIFIABILITY OF LATENT CONCEPTS FROM OBSERVATIONS

Consider any level l in the hierarchy. The concepts \mathbf{S}_{l+1} at the next level are sampled based on \mathbf{S}_l via a generating function $\mathbf{S}_{l+1} = f_{\mathbf{S}_{l+1}}(\mathbf{S}_l, \epsilon_l)$, where ϵ_l denotes the exogenous variables injected into level $l+1$, independent of \mathbf{S}_l and all variables at higher levels. The final response \mathbf{R} can be expressed as \mathbf{S}_l and the collection of exogenous variables $\mathbf{E}_l := (\epsilon_m)_{m=l}^L$ via an invertible function $\mathbf{R} = q_l(\mathbf{S}_l, \mathbf{E}_l)$.

The following lemma shows how the hierarchically-dependent latent concepts \mathbf{S}_{l+1} can be disentangled from the independent exogenous variables \mathbf{E}_{l+1} for any $0 \leq l < L$. The proof is inspired by previous work (Hyvarinen & Morioka, 2016; Hyvarinen et al., 2019; Kong et al., 2022).

Lemma B.1 (Single-level Subspace Identifiability). *Assume the following data-generating process at a fixed, arbitrary $0 \leq l < L$:*

$$\mathbf{S}_{l+1} \sim \mathbb{P}[\mathbf{S}_{l+1} | \mathbf{S}_l], \mathbf{E}_{l+1} \sim \mathbb{P}[\mathbf{E}_{l+1}], \mathbf{R} := q_{l+1}(\mathbf{S}_{l+1}, \mathbf{E}_{l+1}). \quad (5)$$

We have the following conditions.

i **Informativeness:** The function $q_{l+1}(\cdot)$ is a diffeomorphism.

ii **Smooth Density:** The probability density function $p(\mathbf{S}_{l+1}, \mathbf{E}_{l+1} | \mathbf{S}_l)$ is smooth.

iii **Sufficient Variability:** At any value \mathbf{S}_{l+1} , there exist $n(\mathbf{S}_{l+1}) + 1$ distinct values of \mathbf{S}_l , denoted as $\{\mathbf{S}_l^{(n)}\}_{n=0}^{n(\mathbf{S}_{l+1})}$, such that the vectors $\mathbf{w}(\mathbf{S}_{l+1}, \mathbf{S}_l^n) - \mathbf{w}(\mathbf{S}_{l+1}, \mathbf{S}_l^0)$ are linearly independent where $\mathbf{w}(\mathbf{S}_{l+1}, \mathbf{S}_l) = \left(\frac{\partial \log p(\mathbf{S}_{l+1} | \mathbf{S}_l)}{\partial \mathbf{S}_{l+1,1}}, \dots, \frac{\partial \log p(\mathbf{S}_{l+1} | \mathbf{S}_l)}{\partial \mathbf{S}_{l+1,n(\mathbf{S}_{l+1})}} \right)$

If a model θ satisfies i,ii, and iii, another model $\hat{\theta}$ satisfies i,ii, and they generate identical distributions $\mathbb{P}[\mathbf{R} | \mathbf{S}_l] = \hat{\mathbb{P}}[\mathbf{R} | \mathbf{S}_l]$, then the latent concepts \mathbf{S}_{l+1} are identifiable up to an invertible map, disentangled from \mathbf{E}_{l+1} : there exists an invertible mapping $\mathbf{S}_{l+1} \mapsto \hat{\mathbf{S}}_{l+1}$ where \mathbf{S}_{l+1} and $\hat{\mathbf{S}}_{l+1}$ are generated in model θ and $\hat{\theta}$ respectively.

Proof. Since we have matched distributions, it follows that:

$$p(\mathbf{R} | \mathbf{S}_l) = \hat{p}(\mathbf{R} | \mathbf{S}_l). \quad (6)$$

As the generating function q_{l+1} has a smooth inverse (i), we can derive:

$$\begin{aligned} p(q_{l+1}(\mathbf{S}_{l+1}, \mathbf{E}_{l+1}) | \mathbf{S}_l) &= p(\hat{q}_{l+1}(\hat{\mathbf{S}}_{l+1}, \hat{\mathbf{E}}_{l+1}) | \mathbf{S}_l) \implies \\ p(\mathbf{S}_{l+1}, \mathbf{E}_{l+1} | \mathbf{S}_l) \left| \mathbf{J}_{q_{l+1}^{-1}} \right| &= \hat{p}(q_{l+1}^{-1} \circ \hat{q}_{l+1}(\hat{\mathbf{S}}_{l+1}, \hat{\mathbf{E}}_{l+1}) | \mathbf{S}_l) \left| \mathbf{J}_{q_{l+1}^{-1}} \right|. \end{aligned}$$

Notice that the Jacobian determinant $\left| \mathbf{J}_{q_{l+1}^{-1}} \right| > 0$ because of $q_{l+1}(\cdot)$'s invertibility and let $h := q_{l+1}^{-1} \circ \hat{q}_{l+1} : (\hat{\mathbf{S}}_{l+1}, \hat{\mathbf{E}}_{l+1}) \mapsto (\mathbf{S}_{l+1}, \mathbf{E}_{l+1})$ which is smooth and has a smooth inverse thanks to those properties of q_{l+1} and \hat{q}_{l+1} . It follows that

$$\begin{aligned} p(\mathbf{S}_{l+1}, \mathbf{E}_{l+1} | \mathbf{S}_l) &= \hat{p}(h(\hat{\mathbf{S}}_{l+1}, \hat{\mathbf{E}}_{l+1}) | \mathbf{S}_l) \implies \\ p(\mathbf{S}_{l+1}, \mathbf{E}_{l+1} | \mathbf{S}_l) &= \hat{p}(\hat{\mathbf{S}}_{l+1}, \hat{\mathbf{E}}_{l+1} | \mathbf{S}_l) \left| \mathbf{J}_{h^{-1}} \right|. \end{aligned}$$

756 The independence relation in the generating process implies that
 757

$$758 \log p(\mathbf{S}_{l+1}|\mathbf{S}_l) + \sum_{i \in [n(\mathbf{E}_{l+1})]} \log p(\mathbf{E}_{l+1,i}) = \log \hat{p}(\hat{\mathbf{S}}_{l+1}|\mathbf{S}_l) + \sum_{i \in [n(\hat{\mathbf{E}}_{l+1})]} \log \hat{p}(\hat{\mathbf{E}}_{l+1,i}) + \log |\mathbf{J}_{h^{-1}}|. \\ 759 \\ 760 \\ 761$$
(7)

762 For any realization \mathbf{S}_l^0 , we subtract (7) at any $\mathbf{S}_l \neq \mathbf{S}_l^0$ with that at \mathbf{S}_l^0 :

$$763 \log p(\mathbf{S}_{l+1}|\mathbf{S}_l) - \log p(\mathbf{S}_{l+1}|\mathbf{S}_l^0) = \log \hat{p}(\hat{\mathbf{S}}_{l+1}|\mathbf{S}_l) - \log \hat{p}(\hat{\mathbf{S}}_{l+1}|\mathbf{S}_l^0). \\ 764$$
(8)

765 Taking derivative w.r.t. $\hat{\mathbf{E}}_{l+1,j}$ for $j \in [n(\hat{\mathbf{E}}_{l+1})]$ yields:

$$766 \sum_{i \in [n(\mathbf{S}_{l+1})]} \frac{\partial}{\partial \mathbf{S}_{l+1,i}} (\log p(\mathbf{S}_{l+1}|\mathbf{S}_l) - \log p(\mathbf{S}_{l+1}|\mathbf{S}_l^0)) \cdot \frac{\partial \mathbf{S}_{l+1,i}}{\partial \hat{\mathbf{E}}_{l+1,j}} = 0. \\ 767 \\ 768$$
(9)

769 The left-hand side zeros out because $\hat{\mathbf{S}}_{l+1}$ is not a function of $\hat{\mathbf{E}}_{l+1}$.
 770

771 Condition iii ensures the existence of at least $n(\mathbf{S}_{l+1})$ such equations with $\mathbf{S}_l^1, \dots, \mathbf{S}_l^{n(\mathbf{S}_{l+1})}$ that are
 772 linearly independent, constituting a full-rank linear system. Since the choice of $j \in [n(\mathbf{E}_{l+1})]$ is
 773 arbitrary. It follows that

$$774 \frac{\partial \mathbf{S}_{l+1,i}}{\partial \hat{\mathbf{E}}_{l+1,j}} = 0, \forall i \in [n(\mathbf{S}_{l+1})], j \in [n(\mathbf{E}_{l+1})]. \\ 775 \\ 776$$
(10)

777 Therefore, the Jacobian matrix \mathbf{J}_h is of the following structure:

$$778 \mathbf{J}_h = \begin{bmatrix} \frac{\partial \mathbf{E}_{l+1}}{\partial \hat{\mathbf{E}}_{l+1}} & \frac{\partial \mathbf{E}_{l+1}}{\partial \hat{\mathbf{S}}_{l+1}} \\ \frac{\partial \mathbf{S}_{l+1}}{\partial \hat{\mathbf{E}}_{l+1}} & \frac{\partial \mathbf{S}_{l+1}}{\partial \hat{\mathbf{S}}_{l+1}} \end{bmatrix}. \\ 779 \\ 780 \\ 781 \\ 782 \\ 783$$
(11)

784 (10) suggests that the block $\frac{\partial \mathbf{S}_{l+1}}{\partial \hat{\mathbf{E}}_{l+1}} = 0$. Since \mathbf{J}_h is full-rank, we can deduce that $\frac{\partial \mathbf{S}_{l+1}}{\partial \hat{\mathbf{S}}_{l+1}}$ must have
 785 full row-rank and $n(\mathbf{S}_{l+1}) \leq n(\hat{\mathbf{S}}_{l+1})$. Assuming the dimensions of the latent spaces are equal,
 786 $n(\mathbf{S}_{l+1}) = n(\hat{\mathbf{S}}_{l+1})$. Moreover, since \mathbf{J}_h is full-rank and the block $\frac{\partial \mathbf{S}_{l+1}}{\partial \hat{\mathbf{E}}_{l+1}}$ is zero, we can derive
 787 that the corresponding block $\frac{\partial \hat{\mathbf{S}}_{l+1}}{\partial \hat{\mathbf{E}}_{l+1}}$ in its inverse matrix $\mathbf{J}_{h^{-1}}$ is also zero. Therefore, there exists an
 788 invertible map $\mathbf{S}_{l+1} \mapsto \hat{\mathbf{S}}_{l+1}$, which concludes the proof. □
 789

790 With Lemma B.1 in hand, we can prove the following lemma that refines subspace invertible
 791 mappings $\mathbf{S}_{l+1} \mapsto \hat{\mathbf{S}}_{l+1}$ into component-wise invertible mappings $\mathbf{S}_{l+1,i} \mapsto \hat{\mathbf{S}}_{l+1,i}$. That is, one can
 792 identify single dimensions on the level l .
 793

794 To formalize our theoretical results, we introduce the following notation. For a matrix M , we denote
 795 its i -th row and j -th column as $M_{i,\cdot}$ and $M_{\cdot,j}$ respectively. We use \cdot to indicate all the indices in
 796 that dimension. Recall the definition $\mathbf{S}_{l+1} := f_{l+1}(\mathbf{S}_l, \epsilon_l)$ and $\mathbf{R} := q_{l+1}(\mathbf{S}_{l+1}, \mathbf{E}_{l+1})$. We denote
 797 $D_{\mathbf{S}_l} f_{\mathbf{S}_{l+1}}$ as the partial derivative of the function $f_{\mathbf{S}_{l+1}}$ with respect to the higher-level variables \mathbf{S}_l .
 798 Let \mathbf{T} be an arbitrary, fixed matrix with the same support as the matrix-valued function $\mathbf{T}(\cdot)$ in the
 799 relationship between two models' Jacobians: $D_{\mathbf{S}_l} f_{\mathbf{S}_{l+1}} = \mathbf{T} D_{\mathbf{S}_l} f_{\mathbf{S}_{l+1}}$. Given a subset of indices
 800 $\mathcal{S} \subseteq \{1, \dots, n\}$, we define the subspace $\mathbb{R}_{\mathcal{S}}^n$ as $\{s \in \mathbb{R}^n \mid s_i = 0 \text{ if } i \notin \mathcal{S}\}$. The support of the
 801 generative process for level $l+1$ is defined as $\mathcal{D}_l := \text{supp}(D_{\mathbf{S}_l} f_{\mathbf{S}_{l+1}})$. The dependency structure
 802 is captured by a binary matrix M_l , where $M_{l,i,j} = 1$ if and only if $(i, j) \in \mathcal{D}_l$. Let \mathcal{A}_k be the set of
 803 indices for variables in \mathbf{S}_{l+1} that depend on the higher-level variable $\mathbf{S}_{l,k}$. Let $d(\mathbf{S}_l)$ represent the
 804 dimensionality of \mathbf{S}_l . The following conditions follow prior work Zheng et al. (2025; 2022).

805 **Assumption B.2** (Non-degenerative Subspace Zheng et al. (2022)). *Suppose two alternative models
 806 θ and $\hat{\theta}$, with an ℓ_0 regularization on $D_{\mathbf{S}_l} f_{\mathbf{S}_{l+1}}$ such that $|\hat{\mathcal{D}}_l| \leq |\mathcal{D}_l|$, there exists a set of points
 807 $\{(\mathbf{S}_l, \theta)^{(\ell)}\}_{\ell=1}^{|\mathcal{D}_{l,i}|}$ for each $\mathbf{S}_{l+1,i}$, such that:*

808 1. The vectors $\{D_{\mathbf{S}_l} f_{\mathbf{S}_{l+1}}((\mathbf{S}_l, \theta)^{(\ell)}))_{\cdot,i}\}_{\ell=1}^{|\mathcal{D}_{l,i}|}$ are linearly independent.

810 2. The transformed vectors lie in a subspace: $[\mathbf{T}D_{\mathbf{S}_l} f_{\mathbf{S}_{l+1}}((\mathbf{S}_l, \theta)^{(\ell)})]_{\cdot, i} \in \mathbb{R}_{\hat{\mathcal{D}}_{l,\cdot,i}}^{n(\mathbf{S}_{l+1})}$.
 811

812 We adapt a theoretical result from Zheng et al. (2025) as the following lemma.
 813

814 **Lemma B.3** (Pair-wise Identification (Zheng et al., 2025)). *Let $\theta := (f_{\mathbf{S}_{l+1}}, q_{\mathbf{S}_{l+1}})$ and $\hat{\theta} := (\hat{f}_{\mathbf{S}_{l+1}}, \hat{q}_{\mathbf{S}_{l+1}})$ be two alternative models. Suppose θ satisfies Condition B.1-i,ii, and Condition B.2, and $\hat{\theta}$ satisfies Condition B.1-i,ii, and an ℓ_0 constraint $\min \|\text{supp } D_{\hat{\mathbf{S}}_l} \hat{f}_{\mathbf{S}_{l+1}}\|_0$. If θ and $\hat{\theta}$ are observationally equivalent, i.e., $\mathbb{P}[\mathbf{R}|\mathbf{S}_l] = \hat{\mathbb{P}}[\mathbf{R}|\mathbf{S}_l]$ for all \mathbf{S}_l . Then, the Jacobian of the transformation between the latent spaces satisfies:*

$$820 \quad \frac{\partial \hat{\mathbf{S}}_{l+1, \pi(\mathcal{A}_i \setminus \mathcal{A}_j)}}{\partial \mathbf{S}_{l+1, \mathcal{A}_j}} = \mathbf{0} \quad \text{and} \quad \frac{\partial \hat{\mathbf{S}}_{l+1, \pi(\mathcal{A}_j \setminus \mathcal{A}_i)}}{\partial \mathbf{S}_{l+1, \mathcal{A}_i}} = \mathbf{0}, \quad (12)$$

823 where π is a permutation of the variable indices.
 824

825 **Assumption B.4** (Structural Diversity (Zheng et al., 2025)). *For any index i of the variable \mathbf{S}_{l+1} ,
 826 there exists a nonempty index set J and a specific index $j \in J$ for \mathbf{S}_l such that i is the unique index
 827 in \mathcal{A}_j that satisfies $\{i\} = \mathcal{A}_j \setminus \cup_{k \in J \setminus \{j\}} \mathcal{A}_k$. Moreover, the union $\cup_{k \in J} \mathcal{A}_k$ is equal to the entire
 828 index space $[d(\mathbf{S}_l)]$.*

829 **Lemma B.5** (Single-level Component-wise Identifiability). *Let $\theta := (f_{\mathbf{S}_{l+1}}, q_{\mathbf{S}_{l+1}})$ and $\hat{\theta} := (\hat{f}_{\mathbf{S}_{l+1}}, \hat{q}_{\mathbf{S}_{l+1}})$ be two alternative models. Suppose θ satisfies Condition B.1-i,ii,iii and Condition B.4, and $\hat{\theta}$ satisfies Condition B.1-i,ii,iii, and a constraint on the support cardinality $\min |\mathcal{D}_{\hat{\mathbf{S}}_l} \hat{f}_{\mathbf{S}_{l+1}}|$. If θ and $\hat{\theta}$ are observationally equivalent, i.e., $\mathbb{P}[\mathbf{R}|\mathbf{S}_l] = \hat{\mathbb{P}}[\mathbf{R}|\mathbf{S}_l]$ for all \mathbf{S}_l , then the variables \mathbf{S}_{l+1} and $\hat{\mathbf{S}}_{l+1}$ are identifiable up to permutations and invertible transformations. Specifically, for any index i , there exists an invertible mapping $S_{l+1,i} \mapsto \hat{S}_{l+1,\pi(i)}$ for a permutation π .*

837 *Proof.* Notice that we have assumed all conditions for Lemma B.1 and Lemma B.3.
 838

839 For any variable index i on the level $l+1$, invoking Lemma B.1 yields that

$$840 \quad \frac{\partial \hat{S}_{l+1, \pi(i)}}{\partial \mathbf{E}_{l+1}} = 0. \quad (13)$$

843 Assumption B.4 suggests the existence of an index j and an index set J ($j \in J$) for the variable \mathbf{S}_l ,
 844 such that the intersection such that i is the only index in \mathcal{A}_j that is unique to \mathcal{A}_j (relative to other
 845 index sets $\{\mathcal{A}_k\}_{k \in J, k \neq j}$). Lemma B.3 implies that

$$847 \quad \frac{\partial \hat{S}_{l+1, \pi(i)}}{\partial \mathbf{S}_{l+1, \cup_{k \in J} \mathcal{A}_k \setminus \{i\}}} = 0. \quad (14)$$

849 Moreover, since $\cup_{k \in J} \mathcal{A}_k = [d(\mathbf{S}_{l+1})]$ (Assumption B.4), we can deduce that

$$851 \quad \frac{\partial \hat{S}_{l+1, \pi(i)}}{\partial \mathbf{S}_{l+1, [d(\mathbf{S}_{l+1})] \setminus \{i\}}} = 0. \quad (15)$$

854 Combining (13) and (15) yields

$$856 \quad \frac{\partial \hat{S}_{l+1, \pi(i)}}{\partial \mathbf{S}_{l+1, [d(\mathbf{S}_{l+1})] \cup [d(\mathbf{E}_{l+1})] \setminus \{i\}}} = 0. \quad (16)$$

859 Recall that the mapping $(\mathbf{S}_{l+1}, \mathbf{E}_{l+1}) \mapsto (\hat{\mathbf{S}}_{l+1}, \hat{\mathbf{E}}_{l+1})$ is invertible. We can deduce from (16) that
 860 the mapping $S_{l+1,i} \mapsto \hat{S}_{l+1,\pi(i)}$ is invertible. Since the choice of $i \in [d(\mathbf{S}_{l+1})]$ is arbitrary, we have
 861 arrived at the desired conclusion. \square

862 Now, we are ready to present the identifiability for the entire hierarchical model. For ease of ex-
 863 position, we consider the question variables \mathbf{Q} as the top-level variable \mathbf{S}_1 .

864 **Theorem B.6** (Identifiability of the Reasoning Hierarchy). *Let $\theta := (f_{\mathbf{S}_{l+1}}, q_{\mathbf{S}_{l+1}})_{l \in [L]}$ and $\hat{\theta} := (f_{\hat{\mathbf{S}}_{l+1}}, \hat{q}_{\hat{\mathbf{S}}_{l+1}})_{l \in [L]}$ be two alternative models. Suppose every two adjacent levels \mathbf{S}_l and \mathbf{S}_{l+1} from θ satisfy Condition B.1-i,ii,iii and Condition B.4, and every two adjacent levels $\hat{\mathbf{S}}_l$ and $\hat{\mathbf{S}}_{l+1}$ from $\hat{\theta}$ satisfy Condition B.1-i,ii,iii, and a constraint on the support cardinality $\min |\mathcal{D}_{\hat{\mathbf{S}}_l} \hat{f}_{\hat{\mathbf{S}}_{l+1}}|$. If θ and $\hat{\theta}$ are observationally equivalent, i.e., $\mathbb{P}[\mathbf{R}|\mathbf{S}_1] = \hat{\mathbb{P}}[\mathbf{R}|\mathbf{S}_1]$, then the variables \mathbf{S}_l and $\hat{\mathbf{S}}_l$ ($l > 1$) are identifiable up to permutations and invertible transformations. Specifically, for any index $l > 1$ and $i \in d(\mathbf{S}_l)$, there exists an invertible mapping $S_{l,i} \mapsto \hat{S}_{l,\pi_l(i)}$ for a permutation π_l .*

873 *Proof.* Our proof is inductive. Theorem B.5 shows that if the variables at level l are identifiable, then
 874 those at the next level, $l + 1$, are also identifiable. Since the top-level \mathbf{S}_1 is given, i.e., the question
 875 \mathbf{Q} , we can derive that all the variables in the hierarchical model are identifiable up to permutation
 876 and invertible transformations. That is, for any index $l > 1$ and $i \in d(\mathbf{S}_l)$, there exists an invertible
 877 mapping $S_{l,i} \mapsto \hat{S}_{l,\pi_l(i)}$ for a level-specific permutation π_l . \square

C IMPLEMENTATION

882 We build our model based on the code repository by diffu-GRPO (Zhao et al., 2025). We apply
 883 GRPO to LLaDA-8B-Instruct (Nie et al., 2025). Following diffu-GRPO, we generate 6 rollouts per
 884 problem with a temperature of 0.9 and perform 12 update iterations per step (for Sudoku, we follow
 885 diffu-GRPO and use a temperature of 0.3 with 8 iterations). The model is trained with LoRA of
 886 rank 128 in 4-bit precision and evaluated in float16 precision. The learning rate is set to 3×10^{-6}
 887 with 600 warm-up steps. During evaluation, we use zero-shot prompting and greedy decoding, with
 888 generation lengths of 128, 256, and 512 tokens, consistent with diffu-GRPO.

889 In order to compute the step-aware reward, we randomly select a timestep during the generation
 890 of rollouts for optimization. At this point, we take the intermediate generations consisting only of
 891 the text tokens that have been produced so far. We then concatenate 64 additional mask tokens
 892 to this partial sequence and feed the extended input back into the model. The model continues the
 893 process by performing iterative denoising based on this new input. Empirically, we find that using 64
 894 mask tokens provides an effective trade-off between efficiency and performance on the benchmark
 895 datasets. After obtaining the outputs, we first compute the accuracy of the original rollouts, which
 896 reflects the correctness of the answers generated from the question alone. Next, we compute the
 897 accuracy of the newly generated answers obtained from the intermediate generations. Finally, we
 898 define the step-aware reward as the difference between these two accuracies, which quantifies the
 899 contribution of the intermediate generations to the final outcome.

D ADDITIONAL EXAMPLES

900 Here are additional responses comparisons for COUNTDOWN dataset.

901
 902
 903
 904
 905
 906
 907
 908
 909
 910
 911
 912
 913
 914
 915
 916
 917

918
919
920
921
922
923
924
925
926
927
928
929
930
931
932
933
934

	<p>Problem: Using only the provided numbers [19,3,5], create an arithmetic expression evaluates to exactly the target number 52</p>		
935 936 937 938 939 940 941 942 943	<p>To reach the target number using the given numbers, we need to consider the operations of addition, subtraction, multiplication, and division. We can start by using the largest number (19) and the smallest number (3) to form a larger number. Then, we can use the remaining number (5) to adjust the result. Finally, we can use the remaining number to adjust the result.</p> <pre></reasoning> <answer> \boxed{19 * 3 - 3 - 3} </answer>< eot_id >< endoftext ></pre>	<p>To reach the target number using the given numbers, we need to consider the operations of addition, subtraction, multiplication, and division. We can start by trying to use the numbers in a way that sums up to the target number. However, since the target number is larger than the sum of the given numbers, we need to use multiplication to reach the target. We try multiplying the given numbers in different combinations. We find that multiplying 19 by 3 gives us exactly the 52.</p> <pre></reasoning> <answer> \boxed{19 * 3} </answer>< eot_id >< endoftext ></pre>	<p>To create an arithmetic expression that evaluates to exactly target number 52 using the numbers 19, 3, and 5, we need to consider the combinations of the operations +, -, *, and /. Let's try a few combinations:</p> <ol style="list-style-type: none"> 1. $19 + 3 - 5$ 2. $19 - 5 * 3$ <p>From the above, we can that $19 * 3 - 5$ works.</p> <pre></reasoning> <answer> \boxed{19 * 3 - 5} </answer>< eot_id >< endoftext ></pre>
944	<p>LLaDA</p> <p>Answer: X</p> <p>Reasoning: X</p>	<p>diffu-GRPO</p> <p>Answer: X</p> <p>Reasoning: X</p>	<p>Ours</p> <p>Answer: ✓</p> <p>Reasoning: ✓</p>
945 946 947 948 949 950 951 952 953	<p>Problem: Using only the provided numbers [37,1,73], create an arithmetic expression evaluates to exactly the target number 37</p>		
	<p>To get the target number 37 using the numbers 37, 1, and 73, we need to find a combination of operations that, when applied to these numbers, result in 37. We can start by considering the simplest operations and see if we can reach the target.</p> <pre></reasoning> <answer> \boxed{73 - 37} </answer>< eot_id >< endoftext ></pre>	<p>To get the target number 37 using the numbers 37, 1, and 73, we need to find a combination of operations that, when applied to these numbers, result in 37. We can start by considering the simplest operations and see if we can reach the target.</p> <pre></reasoning> <answer> \boxed{73 - 37} </answer>< eot_id >< endoftext ></pre>	<p>To create an arithmetic expression that evaluates to exactly the target number 37 using the numbers 37, 1, and 73, we need to consider the operations +, -, *, and /. Let's try different combinations:</p> <ol style="list-style-type: none"> 1. $73 - 37 + 1$ 2. $73 + 1 - 37$ <p>Both of these expressions evaluate to the target number 37. We can choose either one.</p> <pre></reasoning> <answer> \boxed{73 - 37 + 1} </answer>< eot_id >< endoftext ></pre>
954 955 956 957 958 959 960 961 962 963 964 965 966 967 968 969 970 971	<p>LLaDA</p> <p>Answer: X</p> <p>Reasoning: X</p>	<p>diffu-GRPO</p> <p>Answer: X</p> <p>Reasoning: X</p>	<p>Ours</p> <p>Answer: ✓</p> <p>Reasoning: ✓</p>

Figure 10: Comparison of generated responses across models. We observe that LLaDA produces meaningless reasoning steps, while diffu-GRPO generates incorrect reasoning. In contrast, our model correctly answers the question.